Side-effect of ancillary ligand on electron transfer and photodynamics of a dinuclear valence tautomeric complex†

Bao Li,[a] Jun Tao,*[a] Hao-Ling Sun,[b] Osamu Sato,*[b] Rong-Bin Huang[a] and Lan-Sun Zheng[a]

Received (in Cambridge, UK) 22nd January 2008, Accepted 19th February 2008
First published as an Advance Article on the web 13th March 2008
DOI: 10.1039/b801171k

A cobalt complex [{Co(dpqa)}$_2$(dhbq)](PF$_6$)$_3$ (1(PF$_6$)$_3$, dhbq = deprotonated 2,5-dihydroxy-1,4-benzoquinone, dpqa = di(2-pyridylmethyl)-*N*-(quinolin-2-ylmethyl)amine) was prepared and studied by X-ray diffraction, electrochemistry, ESR, thermally and photo-induced magnetic measurements; the results show that the ancillary ligand finely tuned structural factors as well as intermolecular interactions that affect the VT behavior.

Valence tautomeric (VT) complexes refer to those undergoing intramolecular metal–ligand electron transfer accompanying instantaneous spin-crossover, thus existing in chemically different electronic isomers and behaving as bistable molecules[1] in which the energy gaps between two redox-active centers, a metal ion and an electroactive ligand, happen to be appropriate to permit simultaneous electron transfer and spin-crossover.[2] This electronic conversion process is temperature-dependent and entropy-driven and usually controllable *via* external physical parameters, *e.g.* light or pressure.[3] Challenges in this system involve photoinduced VT conversion, metastable state trapping and broad hysteresis,[4] which are essential to practical application of VT molecules, and the past two decades have witnessed great progress in this field.[5]

Though much effort has been made to study the VT complexes, basic factors that experimentally affect intramolecular electron transfer are not yet clear. Pierpont and co-workers found that VT transitions in the [Co(N–N)(Q)$_2$] system could be mainly influenced by the N-donors and the flexibility of the chelate rings of N–N ancillary ligands,[6] while Dei and co-workers found that in the [ML(diox)]Y·(solvent) system, different counterions Y and solvent molecules could also influence the transition temperature.[7] Thus, more examples are desirable for understanding possible factors that influence valence tautomerism. Recently we reported a complex [{Co(tpa)}$_2$(dhbq)](PF$_6$)$_3$ (tpa = tris(2-pyridylmethyl)amine), which exhibited an abrupt VT transition with distinct hysteresis around room temperature,[8] and this prompted us to pursue our studies on VT complexes with more intriguing properties and hope to find out the essential factors that affect VT behavior and photoinduced processes. Here we report the synthesis, structure and properties of a new dinuclear valence tautomeric complex [{Co(dpqa)}$_2$(dhbq)](PF$_6$)$_3$ (**1**(PF$_6$)$_3$).

Block dark-red crystals of complex **1**(PF$_6$)$_3$ were synthesized *via* one-electron oxidation of [{Co(dpqa)}$_2$(dhbq)](PF$_6$)$_2$ that was prepared from the precursor [CoCl(dpqa)]PF$_6$·0.5H$_2$O.‡

X-Ray diffraction study at 93 K reveals that **1**(PF$_6$)$_3$ crystallizes in the orthorhombic space group *Pccn*, and the molecular cation is located on a crystallographic center of symmetry (Fig. 1(a)).§ **1**$^{3+}$ comprises two ancillary polyamine-chelated Co atoms that are linked by a dhbq bridge, with each Co ion in distorted octahedral geometry, coordinated by two oxygen atoms from dhbq and four nitrogen atoms from dpqa, respectively. The average Co–O and Co–N distances are 1.902 and 1.957 Å in accordance with the typical lengths of low-spin (*ls*) Co^{III}–O[9] and Co^{III}–N,[10] respectively, indicating that the two cobalt ions are Co^{III}. It is of note that both Co–O and Co–N distances are a little longer than those in [{Co(tpa)}$_2$(dhbq)](PF$_6$)$_3$ due to the larger steric hindrance of the quinoline group of dpqa.[8] The C–O1 and C–O2 distances are 1.296(7) and 1.315(6) Å, respectively, which lie between the values of coordinated benzosemiquinonate (1.29 Å) and catecholate (1.35 Å) ligands,[11] indicating the dhbq ligand is a dhbq$^{\bullet 3-}$ radical, though not as conjugated as that in [{Co(tpa)}$_2$(dhbq)](PF$_6$)$_3$.[8] The intramolecular Co···Co distance is 7.521(1) Å, near to those in [{Co(tpa)}$_2$(dhbq)](PF$_6$)$_3$ (7.497(1) Å) and [{Co^{III}(tpa)$_2$(CA$^{\bullet 3-}$)](BF$_4$)$_3$·4MeCN (CA = chloranilate) (7.470(1) Å).[12] Thus, from the structural point of view, **1**$^{3+}$ can be assigned to [(dpqa)Co^{III}–dhbq$^{\bullet 3-}$–Co^{III}(dpqa)]$^{3+}$.

In the solid state, **1**(PF$_6$)$_3$ features a three-dimensional structure (Fig. S1, ESI†) that is formed with alternating layers of **1**$^{3+}$ and counterions, and the layer is characterized by extended networks with C–H···π and π···π interactions (Fig. 1(b)). In the two-dimensional network, the C–H···π_{dhbq} interaction (3.693 Å) comes from the 3-position of pyridyl group and dhbq ligand, and the C–H···π_{py} interaction is somewhat weaker (4.089 Å). The distances between pyridyl and pyridyl groups (centroid···centroid) of π_{py}···π_{py} interactions are 4.172 and 4.601 Å, respectively, and an additional π_{py}···$\pi_{benzene}$ interaction (3.842 Å) is found to be stronger than the other π···π interactions.

The CV of **1**(PF$_6$)$_3$ exhibits three reduction waves (Fig. S2, ESI†) at 0.379, 0.02 and −0.856 V *vs.* SCE, close to those of [{Co^{III}(tpa)}$_2$(CA$^{\bullet 3-}$)](BF$_4$)$_3$·4MeCN.[12] The former two could be assigned to successive one-electron reductions of Co^{III}, and the last one as a two-electron reduction of the dhbq ligand. The reactions in the redox process are expressed by the redox couples of **1**$^{3+}$/**1**$^{2+}$, **1**$^{2+}$/**1**$^{+}$ and **1**$^{+}$/**1**$^{-}$.[11,12] [{Co(tpa)}$_2$(dhbq)](PF$_6$)$_3$

[a] *State Key Laboratory for Physical Chemistry of Solid Surfaces and Department of Chemistry, Xiamen University, Xiamen 361005, People's Republic of China. E-mail: taojun@xmu.edu.cn*
[b] *Institute for Materials Chemistry and Engineering, Kyushu University, Kasuga, 816-8590 Fukuoka, Japan. E-mail: sato@cm.kyushu-u.ac.jp*

† Electronic supplementary information (ESI) available: Fig. S1–S5, Table S1, IR spectra at room temperature, and X-ray crystallographic data. CCDC 675170. For crystallographic data in CIF or other electronic format see DOI: 10.1039/b801171k

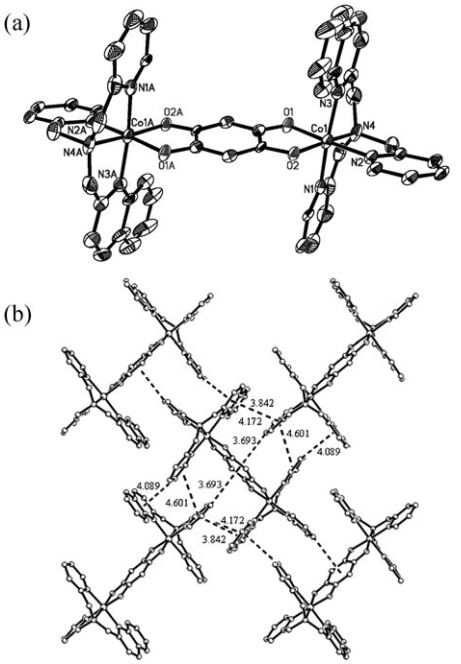

Fig. 1 (a) ORTEP drawing of the structure of $\mathbf{1}^{3+}$ at 35% probability with atom labels. (b) Two-dimensional network of $\mathbf{1}^{3+}$ showing intermolecular interactions.

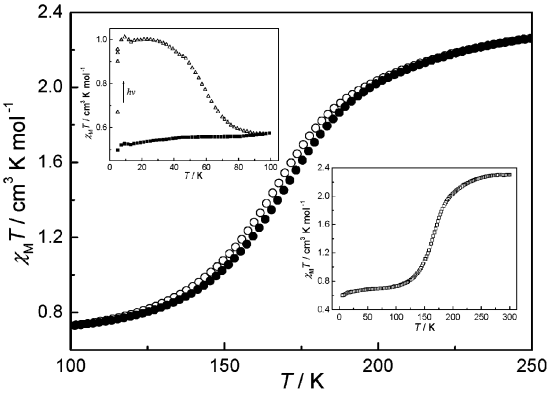

Fig. 2 $\chi_M T$ *vs.* T plots of $\mathbf{1}(PF_6)_3$ showing thermal hysteresis and photo-induced magnetization (top inset).

was also studied and three waves appeared at 0.278, −0.05 and −0.895 V, indicating that the one-electron oxidation from $\mathbf{1}^{2+}$ to $\mathbf{1}^{3+}$ would be more difficult than that from $[\{Co(tpa)\}_2(dhbq)]^{2+}$ to $[\{Co(tpa)\}_2(dhbq)]^{3+}$. The second reductions in both complexes are nearly irreversible, the reasons are not yet clear.

ESR spectra were measured from 100 to 300 K (Fig. S3, ESI†). The strong signal at $g = 2.00$ at 100 K decreases gradually with increasing temperature, which represents the fraction of $dhbq^{\bullet 3-}$ radical formed *via* electron transfer from *hs*-Co^{II} (*hs* = high spin) to $dhbq^{2-}$ at low temperature, decreases when temperature increases due to the occurrence of reverse electron transfer from $dhbq^{\bullet 3-}$ to *ls*-Co^{III}, as in a Co^{III}-semiquinonate complex.[6a] The radical signal disappears at room temperature, implying complete VT conversion at this temperature.

The $\chi_M T$ *vs.* T plots of $\mathbf{1}(PF_6)_3$ are shown in Fig. 2. In the whole temperature range (Fig. 2, bottom inset), the VT interconversion resembles that of $[Co(cth)_2(dhbq)](PF_6)_3$,[13] that is, the $Co^{III}(ls)$–$dhbq^{\bullet 3-}$–$Co^{III}(ls)$ ↔ $Co^{III}(ls)$–$dhbq^{2-}$–$Co^{II}(hs)$ interconversion would be nearly complete. This can be confirmed from the room- and low-temperature $\chi_M T$ values; the $\chi_M T$ value at 300 K reached a saturated value of 2.30 cm^3 K mol^{-1}, similar to those of other VT complexes,[6c] higher than that of $[\{Co(tpa)\}_2(dhbq)](PF_6)_3$ but a little lower than that of a normal *hs*-Co^{II} ion at room temperature. At 5 K, the $\chi_M T$ value of 0.609 cm^3 mol^{-1} K is higher than that of a single $S = 1/2$ semiquinone ligand, which may be due to a paramagnetic impurity. The VT transitions occur at $T_{1/2}\uparrow$ = 171 K and $T_{1/2}\downarrow$ = 168 K, respectively, with almost negligible hysteresis (3 K).

Photo-induced VT transition behavior is shown in Fig. 2 (top inset). After illumination with 532 nm light for 30 min at 5 K, the $\chi_M T$ value increased from 0.60 to 0.96 cm^3 K mol^{-1} to achieve almost saturation value, featuring apparent electron transfer from $dhbq^{\bullet 3-}$ radical to *ls*-Co^{III} ion. The efficiency of photo-induced excitation is about 25%, higher than its tpa analogue.[8] When the light was switched off and the sample was heated at 1 K min^{-1}, it was interesting to find that the $\chi_M T$ value increased gently to 1.01 cm^3 K mol^{-1} at about 10 K, remained almost unchanged from 10 to 23 K, and then gradually decreased to recover to the thermally controlled value at about 97 K, which indicates that the conversion of $Co^{III}(ls)$–$dhbq^{\bullet 3-}$–$Co^{III}(ls)$ ↔ $Co^{III}(ls)$–$dhbq^{2-}$–$Co^{II}(hs)$ is photoswitchable. The upsurge of $\chi_M T$ value after illumination at 10 K is mostly ascribed to the zero field splitting effect of the $S = 3/2$ *hs*-Co^{II} ions.[14] Here, it is worth noting that the existence of a platform in the $\chi_M T$ *vs.* T plots implies the light-induced excited state would be to some extent stable at low temperature, as for the LIEEST phenomena found in spin-crossover complexes,[15] which reveals that the dpqa ligand should be more suitable to trap the excited state than tpa ligand, thus presenting longer relaxation time.

To further investigate the photo-induced excited state species, the temperature-dependent *hs* → *ls* relaxation of the converted high-spin fraction after irradiation was studied and shown in Fig. 3 (from 10 to 70 K), the molar fraction of metastable species was deduced from the equation[16] $\gamma(t) = [(M(t) - M^0)/(M(0) - M^0)] \times 100\%$, where $M(t)$ is the magnetization measured at time t after illumination, $M(0)$ is the magnetization measured at time zero once the light was switched off and M^0 is the magnetization value before illumination. It is found that below 30 K the photo-excited metastable species persists at a level of 90% after 360 min. The shape of the relaxation curve is satisfied with the typical character of VT relaxation, and the relaxation rate constants were calculated by fitting the data with function $\gamma(t) = \gamma^0 \exp(-(K_{VT}(T)t))^{\beta}$, where γ^0 is the converted molar fraction at $t = 0$, $K_{VT}(T)$ is the rate constant of VT relaxation at temperature T, t is the relaxation time and β is a parameter varying from 0 to 1 accounting for the distribution of relaxation times. When $\beta = 0.5$, the data could be well fitted to give relaxation constants $K_{VT}(T)$ for each temperature (Table S1, ESI†). At 70 K, the *hs* → *ls* relaxation corresponds to *ca.* 40% and $K_{VT}(T)$ equals to 4.3×10^{-5} s^{-1}, which is larger than that at low temperature. Fig. S4, ESI† presents the $\ln[K_{VT}(T)]$ *vs.* $1/T$ plot, from 5 to 20 K, that gives an almost straight line with near-zero slope, from which a temperature independent pre-exponential factor $K_{VT}^0 = 6.00 \times 10^{-7}$ s^{-1} could be obtained. The thermally activated relaxation behavior obeying the Arrhenius law could be observed from 30 to 70 K, where the $\ln K_{VT}(T)$ and $1/T$ plots feature a linear

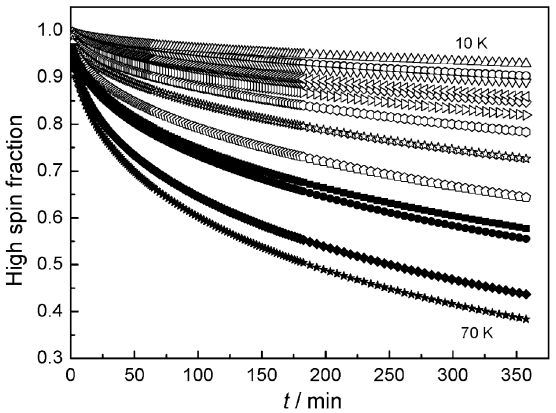

Fig. 3 VT relaxation of the molar fraction of photo-excited metastable $\mathbf{1}(PF_6)_3$ at various temperatures (5 K intervals from 10 to 70 K).

relationship that gives a thermal activation factor $K^0_{VT} = 1.12 \times 10^{-3}$ s^{-1} and activation energy $E_a = 134.77$ cm^{-1}.

At low temperature, the K^0_{VT} value is much smaller than that of $[Co_2(cth)_2(dhbq)](PF_6)_3$ (1.7×10^{-4} s^{-1}),[13] and the activation energy E_a is also lower than the expected value determined by the cobalt–oxygen fully symmetric breathing mode.[17] As hypothesized for the low activation energy E_a at low temperature, the phonon lattice vibration modes[18] may affect the relaxation mechanism by coupling with the ground level vibration mode to determine the tunneling, thus the relaxation time of the photo-induced metastable could be prolonged by increasing the intermolecular interactions. From this point of view, π–π and C–H···π interactions in $\mathbf{1}(PF_6)_3$ would chemically influence the relaxation processes of the metastable species, giving much longer relaxation times than $[\{Co(tpa)\}_2(dhbq)](PF_6)_3$ (Fig. S5, ESI†) and other VT complexes.[16,19]

In conclusion, we have realized thermal and photo-induced VT interconversion in a new complex, whose temperature region holding the metastable species could be chemically enlarged by cooperative intermolecular interactions. The relaxation kinetics of the photo-induced metastable state was characterized by using a first-order stretched exponential decay law to account for the extra long relaxation time.

This work was supported by the NNSF of China (Grant 20671079, 20721001 & 20423002), the Key Project of MOE (Grant 107068) and the 973 project of MSTC (Grant 2007CB815301).

Notes and references

‡ *Synthesis* of $[\{Co(dpqa)\}_2(dhbq)](PF_6)_3$ ($\mathbf{1}(PF_6)_3$). To a well-stirred methanol solution (20 mL) containing dpqa (2.02 mmol) and $CoCl_2 \cdot 6H_2O$ (2.0 mmol) was added an aqueous solution (10 mL) of KPF_6 (5.0 mmol). Green microcrystals of $[CoCl(dpqa)]PF_6 \cdot 0.5H_2O$ precipitated and were filtered by sanction, washed with water and methanol several times. Yield: ~80%. $[CoCl(dpqa)]PF_6 \cdot 0.5H_2O$ (0.2 mmol) was dissolved in a warm methanol solution (15 mL) and a methanol (5 mL) solution containing 2,5-dihydroxy-1,4-benzoquinone (0.1 mmol) and triethylamine (28 μL) was added within 1 min with continuous stirring. After cooling to room temperature and stirring for 15 min, the solution became opaque and red microcrystals of $[\{Co(dpqa)\}_2(dhbq)](PF_6)_2$ precipitated and were filtered by sanction, washed with water and methanol several times. Yield: ~85%. An acetone solution (15 ml) containing $[\{Co(dpqa)\}_2(dhbq)](PF_6)_2$ (0.1 mmol) was added dropwise with an acetone–water (1 : 1, 5 mL) solution containing $AgNO_3$ (0.1 mmol) with stirring, the resulting solution was stirred at room temperature for 30 min, then an aqueous solution (5 mL) of KPF_6 (0.5 mmol) was added and the solution was filtered. Dark-red crystals of $\mathbf{1}(PF_6)_3$ were obtained by slow evaporation of the resulting solution. Yield: ~ 65%. FT-IR (KBr, rt): 3430.15, 1609.0(m), 1550.8(s), 1534.2(sh), 1442.4(w), 1409.0(m), 1384.0(m), 1162.0(w), 840.2(vs), 767.8(w), 559.6(s) cm^{-1}.

§ *Crystal data* for $\mathbf{1}(PF_6)_3$: $C_{50}H_{42}N_8Co_2O_4P_3F_{18}$, $M = 1371.69$, orthorhombic, space group *Pccn*, $Z = 4$. $T = 93(2)$ K, $a = 16.642(3)$, $b = 22.870(5)$, $c = 16.258(3)$ Å, $V = 6188(2)$ Å^3, $D_c = 1.472$ g cm^{-3}, $R_1 = 0.0776$, $wR_2 = 0.1681$, $\mu = 0.715$ mm^{-1}, $S = 0.918$. X-Ray crystallographic data were collected with a Mo-Kα radiation source ($\lambda = 0.71073$ Å) by using Rigaku IP diffractometer equipped with graphite monochromator. The structures were solved by direct methods and refined by full-matrix least-squares calculations (F^2) by using the SHELXTL-97 software. All non-H atoms were refined in the anisotropic approximation against F^2 for all reflections. All H atoms were placed at their calculated positions.

1 *Magnetism: Molecules to Materials II*, ed. J. S. Miller and M. Drillon, Wiley-VCH, Weinheim, 2002, p. 281.
2 P. Gütlich and A. Dei, *Angew. Chem., Int. Ed.*, 1997, **36**, 2734.
3 (*a*) E. Evangelio and D. Ruiz-Molina, *Eur. J. Inorg. Chem.*, 2005, **15**, 2957; (*b*) A. Beni, C. Carbonera, A. Dei, J.-F. Létard, R. Righini, C. Sangregorio and L. Sorace, *J. Braz. Chem. Soc.*, 2006, **17**, 1522; (*c*) O. Sato, A.-L. Cui, R. Matsuda, J. Tao and S. Hayami, *Acc. Chem. Res.*, 2007, **40**, 361; (*d*) O. Sato, J. Tao and Y.-Z. Zhang, *Angew. Chem., Int. Ed.*, 2007, **46**, 2152.
4 (*a*) D. M. Adams, A. Dei, A. L. Rheingold and D. N. Hendrickson, *J. Am. Chem. Soc.*, 1993, **115**, 8221; (*b*) S. H. Bodnar, A. Caneschi, A. Dei, D. A. Shultz and L. Sorace, *Chem. Commun.*, 2001, 2150; (*c*) A. Caneschi, A. Cornia and A. Dei, *Inorg. Chem.*, 1998, **37**, 3419.
5 (*a*) D. M. Adams, A. Dei, A. L. Rheingold and D. N. Hendrickson, *Angew. Chem., Int. Ed.*, 1993, **32**, 880; (*b*) A. Caneschi and A. Dei, *Angew. Chem., Int. Ed.*, 1998, **37**, 3005; (*c*) A. S. Attia, O. S. Jung and C. G. Pierpont, *Inorg. Chim. Acta*, 1994, **226**, 91; (*d*) C. W. Lange, M. Földeàki, V. I. Nevodchikov, G. A. Abakumov and C. G. Pierpont, *J. Am. Chem. Soc.*, 1992, **114**, 4220; (*e*) A. Dei, D. Gatteschi, C. Sangregorio and L. Sorace, *Acc. Chem. Res.*, 2004, **37**, 827.
6 (*a*) R. M. Buchanan and C. G. Pierpont, *J. Am. Chem. Soc.*, 1980, **102**, 4951; (*b*) C. G. Pierpont and R. M. Buchanan, *Coord. Chem. Rev.*, 1981, **38**, 45; (*c*) D. M. Adams and D. N. Hendrickson, *J. Am. Chem. Soc.*, 1996, **118**, 11515; (*d*) O. Sato, S. Hayami, Z.-Z. Gu, T. K. Akahashi, R. Nakajima, K. Seki and A. Fujishima, *J. Photochem. Photobiol., A*, 2002, **149**, 111.
7 A. Caneschi, A. Dei, F. Fabrizi de Biani, P. Gütlich, V. Ksenofontov, G. Levchenko, A. Hoefer and F. Renz, *Chem. Eur. J.*, 2001, **7**, 3926.
8 J. Tao, H. Maruyama and O. Sato, *J. Am. Chem. Soc.*, 2006, **128**, 1790.
9 (*a*) C. G. Pierpont, S. K. Larson and S. R. Boone, *Pure Appl. Chem.*, 1988, **60**, 1331; (*b*) A. Bencini, A. Caneschi, C. Carbonera, A. Dei, D. Gatteschi, R. Righini, C. Sangregorio and J. V. Slageren, *J. Mol. Struct.*, 2003, **656**, 141.
10 (*a*) P. Gütlich, V. Ksenofontov and A. B. Gaspar, *Coord. Chem. Rev.*, 2005, **249**, 1811; (*b*) Spin Crossover in Transition Metal Compounds III, *Top. Curr. Chem.*, ed. P. Gütlich and H. A. Goodwin, Springer, New York, 2004, vol. 235, p. 23.
11 Spin Crossover inTransition Metal Compounds II, *Top. Curr. Chem.*, ed. P. Gütlich and H. A. Goodwin, Springer, New York, 2004, vol. 234, p. 63.
12 K. S. Min, A. G. DiPasquale, J. A. Golen, A. L. Rheingold and J. S. Miller, *J. Am. Chem. Soc.*, 2007, **129**, 2360.
13 C. Carbonera, A. Dei, J.-F. Létard, C. Sangregorio and L. Sorace, *Angew. Chem., Int. Ed.*, 2004, **43**, 3136.
14 A. Bencini, A. Beni, F. Costantino, A. Dei, D. Gatteschi and L. Sorace, *Dalton Trans.*, 2006, 722.
15 M. Yamada, E. Fukumoto and M. Ooidemizu, *Inorg. Chem.*, 2005, **44**, 6967.
16 A.-L. Cui, K. Takahashi, A. Fujishima and O. Sato, *J. Photochem. Photobiol., A*, 2004, **167**, 69.
17 C. Carbonera, A. Dei, J. F. Létard, C. Sangregorio and L. Sorace, *Inorg. Chim. Acta*, 2007, **360**, 3825.
18 Spin Crossover in Transition Metal Compounds I, *Top. Curr. Chem.*, ed. P. Gütlich and H. A. Goodwin, Springer, New York, 2004, vol. 233, p. 49.
19 A. Beni and A. Dei, *Chem. Commun.*, 2007, 2160.